PLOS ONE

RESEARCH ARTICLE

Application of CNTF or FGF-2 increases the number of M2-like macrophages after optic nerve injury in adult *Rana pipiens*

Rosa E. Blanco[1,2]*, Giam S. Vega-Meléndez[1,2], Valeria De La Rosa-Reyes[1,2], Clarissa del Cueto[1], Jonathan M. Blagburn[1]

1 Institute of Neurobiology, University of Puerto Rico Medical Sciences Campus, Old San Juan, Puerto Rico, **2** Department of Anatomy and Neurobiology, University of Puerto Rico School of Medicine, San Juan, Puerto Rico

* rosa.blanco@upr.edu

Citation: Blanco RE, Vega-Meléndez GS, De La Rosa-Reyes V, del Cueto C, Blagburn JM (2019) Application of CNTF or FGF-2 increases the number of M2-like macrophages after optic nerve injury in adult *Rana pipiens*. PLoS ONE 14(5): e0209733. https://doi.org/10.1371/journal.pone.0209733

Editor: Antal Nógrádi, Szegedi Tudomanyegyetem, HUNGARY

Received: December 10, 2018

Accepted: April 17, 2019

Published: May 2, 2019

Data Availability Statement: All relevant data are within the paper and its Supporting Information files.

Funding: REB is supported by grant GM116692 (National Institutes of Health, https://www.nih.gov). JMB is supported by grant GM121190 (National Institutes of Health). GSV-M was supported by GM061838 (Research Initiative for Scientific Enhancement, National Institutes of Health). The Institute of Neurobiology confocal microscopes were funded by DBI 0115825 (National Science

Abstract

We have previously shown that a single application of the growth factors ciliary neurotrophic factor (CNTF) or fibroblast growth factor 2 (FGF-2) to the crushed optic nerve of the frog, *Rana pipiens*, increases the numbers and elongation rate of regenerating retinal ganglion cell axons. Here we investigate the effects of these factors on the numbers and types of macrophages that invade the regeneration zone. In control PBS-treated nerves, many macrophages are present 100 μm distal to the crush site at 1 week after injury; their numbers halve by 2 weeks. A single application of CNTF at the time of injury triples the numbers of macrophages at 1 week, with this increase compared to control being maintained at 2 weeks. Application of FGF-2 is equally effective at 1 week, but the macrophage numbers have fallen to control levels at 2 weeks. Immunostaining with a pan-macrophage marker, ED1, and a marker for M2-like macrophages, Arg-1, showed that the proportion of the putative M2 phenotype remained at approximately 80% with all treatments. Electron microscopy of the macrophages at 1 week shows strong phagocytic activity with all treatments, with many vacuoles containing axon fragments and membrane debris. At 2 weeks with PBS or FGF-2 treatment the remaining macrophages are less phagocytically active, containing mainly lipid inclusions. With CNTF treatment, at 2 weeks many of the more numerous macrophages are still phagocytosing axonal debris, although they also contain lipid inclusions. We conclude that the increase in macrophage influx seen after growth factor application is beneficial for the regenerating axons, probably due to more extensive removal of degenerating distal axons, but also perhaps to secretion of growth-promoting substances.

Introduction

Retinal ganglion cells (RGCs) react to injury in different ways in different groups of animals–for example, mammalian neurons mostly die and the remainder show poor regrowth due to an inhibitory environment [1–4], fish CNS neurons survive and regenerate successfully [5,6],

Foundation https://www.nsf.gov), DoD 52680-RT-ISP (Department of Defense https://cdmrp.army.mil/funding/) and G12 MD007600 (Research Centers for Minority Institutions, National Institutes of Health). The Institute of Neurobiology transmission electron microscope was funded by DBI-0959225 (National Science Foundation). The funders had no role in study design, data collection and analysis, decision to publish, or preparation of the manuscript.

Competing interests: The authors have declared that no competing interests exist.

while amphibian neurons show intermediate survival rates and successful regrowth [7]. RGC death after injury was first thought to be due to interruption of the supply of target-derived neurotrophic factors [1,8–10]. However, addition of these factors has only partial and transient success in saving mammalian RGCs [11,12], although it is highly effective in the frog [13]. More recent work has shown that injury-evoked mammalian RGC death can be largely prevented by inhibition of the leucine zipper kinase pathway [14], by preventing the formation of neurotoxic reactive astrocytes [15], and by eliminating retinal Zn^{2+} accumulation [16].

In recent years, it has been proposed that macrophages play a key role in modulating the progression of neurodegenerative diseases [17–20] and also the response to CNS injury [21–23]. Macrophages originate from bone-marrow-derived monocytes, which circulate in the bloodstream [24] and are then capable of infiltrating injured tissues, where they differentiate into macrophages [25,26]. Along with already-resident microglia, these cells phagocytose debris [27] and secrete chemicals that enhance or inhibit the inflammatory response [28,29]. Macrophage infiltration into the eye after lens injury promotes retinal ganglion cell (RGC) survival and regeneration [30–33]. In the peripheral nervous system also there is strong evidence that the entry of myeloid cells is important for axonal regeneration [27], with their entry being dependent upon the response of the macrophage CCR2 receptor to the cytokine CCL2 [34–36]. However, the potential roles of phagocytic cells in modulating neuronal survival and axonal regrowth after injury remain somewhat ambiguous, in part because of their dual pro- and anti-inflammatory phenotypes [34,37,38].

Our previous work has concentrated on RGC survival after damage to the optic nerve of the frog, *Rana pipiens*, and the beneficial effects of topical growth factor administration upon that survival [13,39–42]. Recently we showed that the speed of RGC axonal regeneration is also increased by a single application of ciliary neurotrophic factor (CNTF) or fibroblast growth factor 2 (FGF-2) [43]. In the course of that study we found large numbers of cells with the ultrastructural characteristics of macrophages that congregated at the injury site, confirming an observation made by our laboratory two decades earlier [44]. From these results, and from previous studies implicating CNTF-induced macrophages in regeneration [33], the question arose as to whether the application of the growth factors could increase the numbers of macrophages present, and it is this question that we address in the present study. The results of these experiments show that application of these growth factors, in particular CNTF, does increase and prolong the numbers of macrophages in the nerve.

Materials and methods

Animals

Adult frogs (*Rana pipiens*) of both sexes were used. They were obtained from Connecticut Valley Biological Supply Company (Southampton, MA) and kept in tanks with recirculating tap water at 19˚C. A total of approximately 50 animals were used for the immunohistochemistry and electron microscopy experiments. This study was carried out in strict accordance with the recommendations in the Guide for the Care and Use of Laboratory Animals of the National Institutes of Health, and the recommendations of the Panel on Euthanasia of the American Veterinary Medical Association. The protocol was approved by the Institutional Animal Care and Use Committee of the University of Puerto Rico Medical Sciences Campus. All surgery was performed under tricaine anesthesia, and all efforts were made to minimize suffering.

Surgical technique for optic nerve crush

With animals under 0.3% tricaine anesthesia, the right eyeball was approached from the palate in which an incision was made; the extraocular muscles were teased aside, and the extracranial

portion of the optic nerve was exposed. Avoiding large blood vessels, the nerve was crushed at the halfway point using Dumont No. 5 forceps. This leaves the meningeal sheath intact but creates a transparent gap that is completely free of axons. We have confirmed the lack of even the smallest of axons in this region by electron microscopic observation; also, crushing in this manner perturbs RGC survival almost as effectively as cutting [13]. The incision was sutured, and the animals were allowed to recover for several hours in the laboratory under observation before replacing them in their tanks in the animal facility.

Neurotrophic factor application

Immediately after the optic nerve was crushed, it was placed on a strip of Parafilm and 5 μl of FGF-2 or CNTF solution was applied directly to the crush lesion. The solution was left in place for 5 min, then the Parafilm was removed and the palate sutured. Control applications consisted of 5 μl of phosphate-buffered saline (PBS: 0.1M). For FGF-2 (R & D Systems, MN, USA) and CNTF (Sigma, St Louis, MO, USA) 125 ng total were applied, dissolved in 5 μl of 0.1M PBS, pH 7.4.

Resin embedding for light and electron microscopy

Animals were euthanized one and two weeks after optic nerve crush and PBS, CNTF, or FGF-2 application (N = 3–6 per treatment). With animals under 1% tricaine + 0.04% $NaHCO_3$ anesthesia, the head of the animal was cut off and the region of the optic nerve was approached from the palate and left in fixative overnight (2% paraformaldehyde + 2% glutaraldehyde in diluted in 0.1 M cacodylate buffer with 0.05% $CaCl_2$). The next day, the samples were washed twice in 0.1 M cacodylate buffer, 5 minutes each. The proximal and distal stumps of the optic nerve and a portion of the eyeball were carefully dissected then postfixed under a fume hood with 1% osmium tetroxide (OsO_4) diluted in cacodylate buffer for 1 h. Subsequently, the samples were dehydrated in 25%, 50%, and 70% ethanol, 5 minutes each, then were placed in 3% uranyl acetate diluted in 70% ethanol for 1 h. The dehydration process was continued, placing the nerves in 90% ethanol (5 minutes), three times in 100% ethanol (20 minutes each), and 10 minutes in propylene oxide. The nerves were infiltrated with 50/50 Epon-Araldite resin and propylene oxide for 1 h, then in 100% Epon-Araldite and left in the desiccator overnight. The next day the nerve samples were placed in cubic molds and embedded in 100% resin, then placed in a 60˚C oven for 24 hours. The resin block was trimmed and, using an ultramicrotome (Sorvall MT-2), transverse sections were cut; semi-thin sections (1 μm thick) for light microscopy, and ultrathin (90 nm) for electron microscopy. For light microscopy, semi-thin sections were stained using methylene blue-azure II and basic fuschin. Thin sections were examined with a JEOL JEM-1011 electron microscope equipped with a Gatan digital camera (Model-832) to describe the ultrastructural features of the nerve.

Light microscopy cell counts

Serial 1 μm resin sections were cut from the optic nerve, starting at the distal stump and working proximally until the injury site was reached, collecting the sections every 50 μm. The section 100 μm distal to the injury site was used for detailed analysis, because many regenerating axons have reached this point at one week [43]. In addition, preliminary cell counts indicated that cells were present at all levels in the nerve, from the crush site to 700 um distal to it, and that the 100 um distance is fairly representative of the cell numbers overall (S1 Table). Composite high magnification light microscope images of the nerve were examined in Adobe Photoshop or GIMP. Image filenames were first coded so as to blind the observer to whether they came from experimental or control animals. Color overlays were constructed by a trained

observer (JMB), outlining the nerve and macrophage-like cell bodies within it. Macrophage cell profiles were identified by their large size, dark cytoplasm, and the presence of granules and/or cytoplasmic vacuoles. It is possible that some of the smallest profiles identified by these criteria may represent phagocytic microglia that are intrinsic to the nerve rather than peripherally-derived macrophages. The overlays were thresholded in ImageJ (Fiji) and cell numbers and sizes were quantified automatically using the Analyze Particles function.

Immunohistochemistry

After dissection, 3–5 eye cups with optic nerves attached were fixed for each control and experimental stage with buffered 2% paraformaldehyde solution for 1 hr. After PBS washing, the tissues were placed in 30% sucrose for cryoprotection at 4˚C overnight, and, after being frozen, cryostat sections of 12–20 μm were cut. After air-drying, sections were immersed in 10 mM citrate buffer (pH 6) for 10 min at 60˚C. The sections were washed twice (5 min each) in PBS containing 0.3% Triton X-100 + 0.5% bovine serum albumin (BSA) and incubated for 30 minutes in the same buffer containing 10% normal goat serum (NGS; for, ED1) or 10% normal rabbit serum (NRS; for Arg1). They were then incubated with the antibodies against ED1 (1:100; catalog # MCA5709; ABD Serotec) and Arginase 1 (1:100; catalog # sc-18355; Santa Cruz Biotechnology), diluted in 0.1M PBS + 0.3% Triton X-100 + 0.5% BSA, overnight at 4˚C. After several washes in the same buffer solution the sections were incubated with goat anti-mouse Cy2 (1:100, Jackson ImmunoResearch Laboratories, Inc.), rabbit anti-goat CY3 (1:100, Jackson ImmunoResearch Laboratories, Inc) for 2 h at room temperature. For ED1 and Arg1 sections, we labeled the cell nuclei with 4',6-diamidino-2-phenylindole (DAPI) staining for 5 minutes after the secondary antibodies. The sections were rinsed in 0.1 M PBS six times, 5 minutes each, and mounted in Polymount.

Omitting the primary antibodies resulted in the absence of immunostaining. The ED1 antibody recognizes rodent and bovine CD68 or macrosialin, which has some homology with amphibian lysosomal proteins. Additionally, a second polyclonal antibody against CD-68 (Abcam #ab124212) gave a very similar staining pattern. The Arg1 polyclonal antibody recognizes the C terminus of mammalian arginase 1, the likely antigenic regions of which show almost 70% identity with amphibian arginase. Because we cannot be completely sure that the antibodies indeed recognize frog homologs of these mammalian proteins, we refer to the staining as "ED1-like immunoreactivity" (ED1-LI) and "Arg1-like immunoreactivity" (Arg1-LI).

Frozen sections of the whole optic nerve processed with ED1 and Arg1 were used to count the macrophages at the injury site. Alternating longitudinal sections through the nerve were analyzed to avoid overlap of data. The number of stained macrophages of each type was counted from confocal images obtained with a Zeiss Pascal laser scanning confocal microscope, using Zeiss LSM5 Image Browser Software, then expressed as a proportion (Arg1/ED1). The statistical significance was determined using ANOVA with *post-hoc* Tukey-Kramer tests ($^{*}P < 0.05$, $^{**}P < 0.01$, $^{***}P < 0.001$).

Electron microscopic analysis of phagocytic structures

Sub-cellular structures ("organelles") indicative of phagocytic activity were quantified from electron micrographs of macrophage cell profiles. These organelles were classified as (1) phagocytic vacuoles, which ranged from 1 to 6 μm in diameter and were electron lucent and contained obvious cellular debris; (2) multilamellar bodies, which ranged from 0.5 to 3 μm in diameter and were composed of multiple electron-dense lamellae or vesicles; and (3) lipid droplets, which ranged from 0.3 to 2 μm in diameter, were generally homogeneously electron-lucent and had no bounding membrane. Organelles of these types were counted and their

areas measured using Fiji in 230 cells from 3 animals per experimental group. The total area of each type of structure per cell was expressed as a percentage of the total area of all the organelles, thus standardizing for variations caused by different cell profile sizes, oblique sections, and partial image cropping. Data were plotted as kernel density ("violin") plots with superimposed box-whisker plots showing the median and 25–75 percent quartiles (box) and minimum/maximum values (whiskers). Since data were not normally distributed the statistical significance was determined using ANOVA with *post-hoc* Mann-Whitney pairwise comparisons using Bonferroni corrected p-values ($^{*}P < 0.05$, $^{**}P < 0.01$, $^{***}P < 0.001$).

Results

Growth factor application increases the numbers of macrophages in the injured optic nerve

Transverse 1 μm resin sections of control optic nerves were examined with light microscopy (Fig 1). We chose to focus on the region 100 μm distal to the crush site because many regenerating axons have reached this point at one week [43]. Macrophages were identified by their

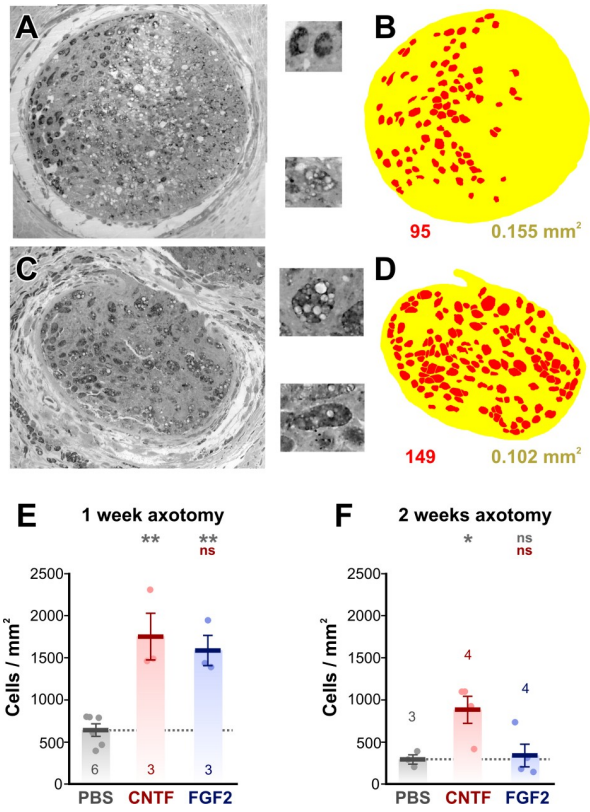

Fig 1. Growth factor treatment increases macrophage numbers. (A and C) Light micrographs of 1 μm resin sections of optic nerves, taken 100 μm distal to the crush zone. A is a PBS-treated control, C is from a CNTF-treated animal. The insets show enlarged examples of macrophage cell profiles, showing dark staining, granules, and vacuoles. (B and D) Color overlays of the light micrographs, delineating macrophage cell profiles (red) and the nerve itself (yellow). The cell count and nerve area derived from these overlays are shown below. (E and F). Combined scatterplots and barcharts of cell density showing mean ± SEM. Asterisks or "ns" above each column indicate the significance when compared to PBS (row 1, gray) or CNTF (row 2, red) with ANOVA and *post-hoc* Tukey tests. (E) At 1 w after nerve crush there are increases in cell density with CNTF and FGF-2 treatment, compared to PBS-treated controls. (F) 2 weeks after crush, only CNTF treatment shows an effect.

https://doi.org/10.1371/journal.pone.0209733.g001

large size, dark staining and granular/vacuolar appearance (Fig 1A and 1C. In PBS-treated controls, from 71 to105 macrophage cell profiles were counted in this region from overlays (Fig 1B, N = 6 animals). Because the cross-sectional area of the nerve varied somewhat between preparations (0.089–0.225 mm^2), this count was converted to cell density, giving a mean of 644 ± 38 cells/mm^2 (N = 6, Fig 1D). Treatment with CNTF increased macrophage cell density 2.7-fold to 1751 ± 481 cells/mm^2 at 1 w (N = 3, Fig 1E). Treatment with FGF-2 was equally effective, increasing cell density 2.5-fold to 1591 ± 309 cells/mm^2 at 1 w (N = 3, Fig 1E).

By two weeks after axotomy the numbers of macrophages in the region 100 μm distal to the crush site was significantly decreased by about half in control PBS-treated animals, to 294 ± 93 cells/mm^2 (N = 3, p = 0.017, homoscedastic t-test). The cell density remained elevated 3-fold with CNTF treatment at 887 ± 323 cells/mm^2 (N = 4, Fig 1F), although this was significantly less than at 1 w (p = 0.035, homoscedastic t-test). However, cell density with FGF-2 treatment had fallen to control levels (342 ± 271 cells/mm^2, N = 4, Fig 1F).

The macrophage overlays allowed the quantification of various parameters of the cell profiles. We were interested to determine whether the cells became larger as a result of growth factor treatment, and so measured their diameter (Feret diameter, ie. longest diameter of each profile). Diameters were segregated in 10 μm bins for each preparation, then these totals were expressed as a percentage of the total number of cells and averaged over the experimental animals (Fig 2). The majority (90%) of the cell profiles fell in the range of 20–40 μm (Fig 2). However, we found no significant changes in cell size as a result of growth factor treatment (ANOVA followed by *post-hoc* Tukey tests), and neither were there any changes in size between 1 week (Fig 2A) and 2 weeks after optic nerve injury (Fig 2B).

Growth factor application does not alter the relative proportions of macrophage types

Macrophages in mammals can be divided into two broad types: pro-inflammatory M1 and alternatively-activated pro-repair M2, which can be distinguished by their expression of different antigenic markers. During spinal cord injury the pro-inflammatory type overwhelms the small, transient, M2 response [22,28]. We were therefore interested to determine whether frog macrophages could be identified as M1 or M2 and to find out whether their relative proportions changed at different times after injury and growth factor treatment.

Longitudinal frozen sections of optic nerves were stained with two antibodies, ED1 and Arg1 (Fig 3). Counterstaining with DAPI showed that most, but not all, cells within the control, PBS-treated optic nerves were ED1-positive (Fig 3A–3D). The ED1 antibody recognizes the mammalian CD68 (macrosialin in mouse) protein, which is expressed in the lysosomes of all macrophages [45–47]. BLAST searches indicated some homology with amphibian lysosomal proteins so it is possible that ED1 also labels a *Rana* homolog of CD68. In any case, it is clear from high magnification images (Fig 3A and 3B) that ED1 does indeed stain lysosome-like structures, confirming its utility as a pan-macrophage marker in amphibia.

The Arg1 antibody recognizes the C terminus of mammalian arginase 1, which is a classical marker for pro-repair M2 macrophages [48]. A BLAST search of the likely antigenic regions of this molecule showed an almost 70% identity with amphibian arginase, making it likely that Arg1 stains arginase, and therefore M2-like macrophages, in *Rana*. We carried out double immunostaining of optic nerve sections using Arg1-like immunoreactivity (Arg1-LI) along with ED1-like immunoreactivity (ED1-LI) to determine how the relative proportion of putative M2 macrophages changed after injury and growth factor treatment (Fig 3). In fact, we found that at 1 week after injury the proportion of Arg1-LI/ED1-LI macrophages was approximately 80% (Fig 3E), and that it remained at this level at 2 weeks after injury (Fig 3F).

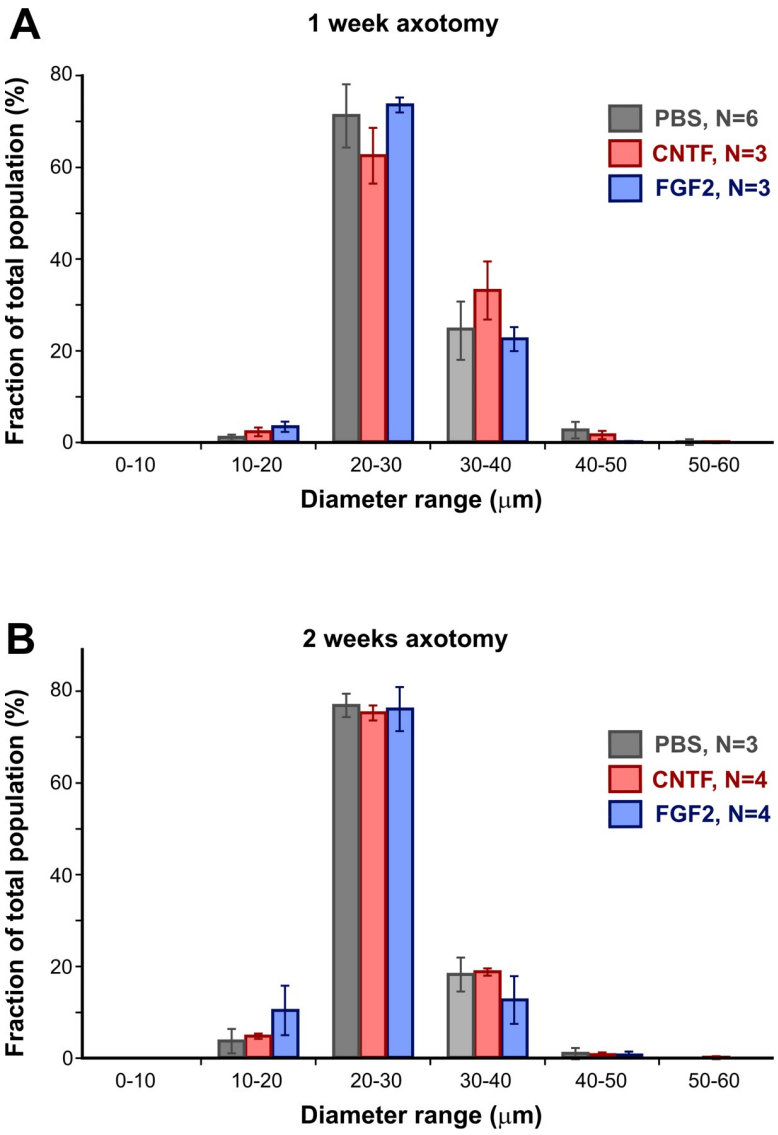

Fig 2. Growth factor treatment does not alter macrophage size. (A and B). Histograms of cell profile diameter (Feret diameter) averaged over several preparations, showing mean ± SEM for each size category. There are no significant differences in cell sizes with growth factor treatment, either at one or two weeks, and no changes in the population of profile diameters between those times.

https://doi.org/10.1371/journal.pone.0209733.g002

Treatment with CNTF or FGF-2 had no effect on the relative proportions of Arg1-LI/ED1-LI macrophages, even though the total numbers were increased (see Fig 1). This result indicates that in *Rana*, unlike rodents, there is a high proportion of putative M2 (pro-repair) macrophages present soon after injury, and that this proportion remains unchanged for at least 2 weeks, during the period when regeneration is taking place [43].

Ultrastructural characteristics of macrophages in the optic nerve after injury

The optic nerve is surrounded by the meningeal sheath, a connective tissue layer that protects the CNS and separates it from the environment. Beneath this is the *glia limitans*, a layer made

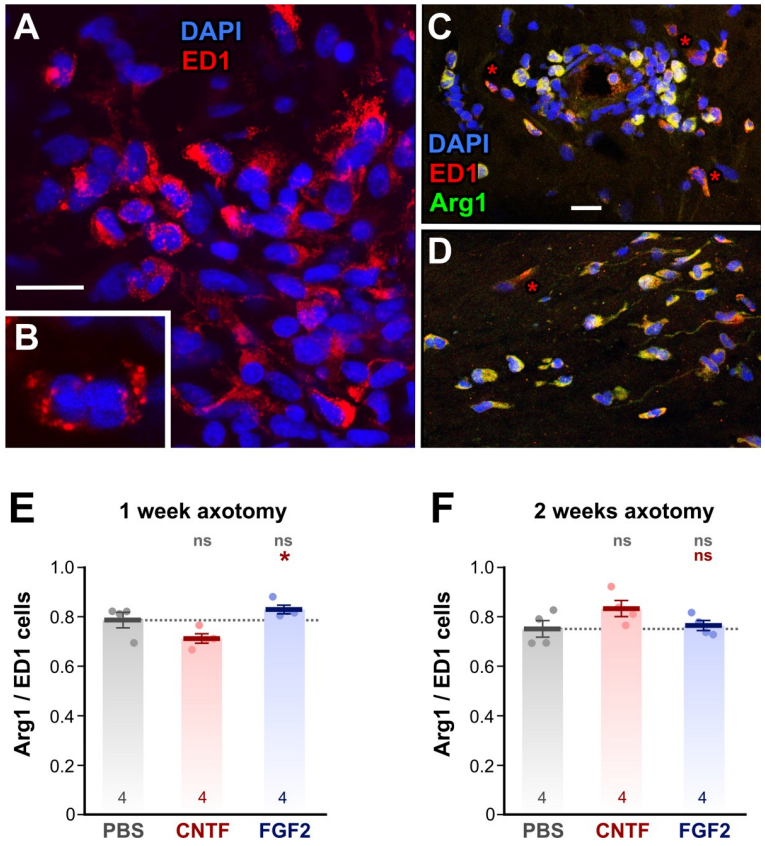

Fig 3. Immunostaining of macrophage subtypes. (A—D) Confocal fluorescence micrographs of immunostained frozen sections of optic nerve 1 week after axotomy. (B) High magnification single slice of a macrophage with an irregular nucleus, clearly showing ED1-LI-stained lysosomes. (C) Double staining of peripherally-located macrophages with ED1 and Arg1. Only a few cells have predominantly ED1-LI with little Arg1-LI (asterisks). (D) Double staining of centrally-located macrophages with ED1 and Arg1. Only a few cells have predominantly ED1-LI (asterisks). (E and F). Combined scatterplots and barcharts of Arg1-LI/ED1-LI ratio showing mean ± SEM. Asterisks or "ns" above each column indicate the significance when compared to PBS (row 1, gray) or CNTF (row 2, red) with ANOVA and *post-hoc* Tukey tests. At 1 w (E) and 2 w (F) after nerve crush there is no change in the Arg1-LI/ED1-LI proportion with CNTF and FGF-2 treatment, compared to PBS-treated controls. Scale bar: 20 μm in A, C, D; 10 μm in B.

https://doi.org/10.1371/journal.pone.0209733.g003

up of astrocytes, glial cells that characteristically exhibit large bundles of intermediate filaments and desmosomes [44]. One week after optic nerve crush, actively phagocytosing macrophages were present inside the optic nerve, presumably playing a role in clearance of the debris (Fig 4). Cells with large vacuoles were common, particularly in central regions of the nerve (Fig 4D). These vacuoles appeared to contain the remnants of degenerating axons and myelin. Other cells contain fewer large vacuoles and more multilamellar and multivesicular bodies (Fig 4E). Two weeks after nerve crush, there appeared to be fewer macrophages in the nerve (Fig 4F and 4G). Those which were present, both peripherally and centrally, contained fewer vacuoles with axonal debris and more, less-electron-dense, homogeneously-stained inclusions which likely represent lipid droplets, since they had no bounding membrane and sometimes showed signs of coalescence (Fig 4F inset).

CNTF treatment prolongs optic nerve macrophage activity

One week after optic nerve injury and treatment with CNTF, large numbers of macrophages were found within the optic nerve, both peripherally (Fig 5A and 5B) and centrally (Fig 5C

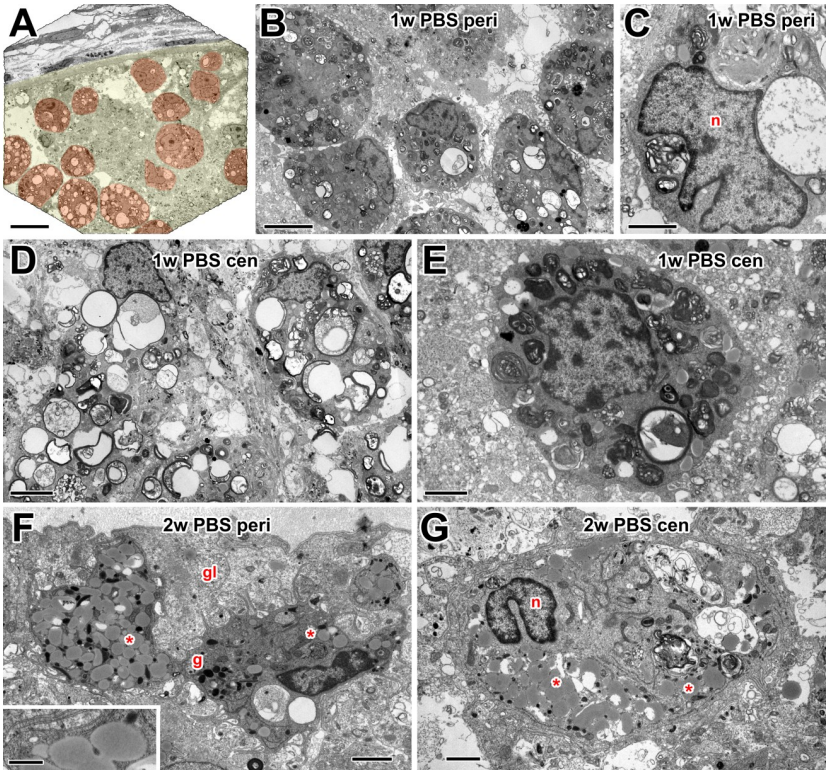

Fig 4. Electron microscopy of macrophages in PBS controls. (A) Low power electron micrograph of the optic nerve periphery at 1 w after injury, with a pale yellow overlay indicating the nerve and pale red overlay indicating numerous macrophages within it. (B) Peripheral macrophages containing a variety of multilamellar and multivesicular bodies, products of phagocytic activity. (C) Macrophage with an irregular nucleus (n) and large debris-filled multilamellar bodies. (D) Centrally located macrophages containing large vacuoles with apparent remnants of degenerating axons. (E) Central, smaller (possibly microglia) cell with multilamellar and multivesicular bodies. (F) Peripheral macrophages at 2 weeks, located within the glia limitans (gl). Some vacuoles with axonal debris are present but the cytoplasm also contains lipid inclusions (asterisks) and dark granules (g). Inset: high magnification view of putative lipid inclusions, showing lack of a bounding membrane. (G) Large central macrophage with a bilobed nucleus (n) at 2 weeks, containing a mixture of vacuoles with axonal debris, and lipid inclusions (asterisks). Scale bar: 20 μm in A; 5 μm in B, D; 2 μm in C, E, F, G; 0.5 μm in inset.

https://doi.org/10.1371/journal.pone.0209733.g004

and 5D). These appeared to be highly active phagocytically, judging by the large numbers and sizes of debris-containing vacuoles and multilamellar bodies. Additionally, other cell types, such as the smaller microglia and neutrophils (Fig 5C) were also occasionally observed. Compared to PBS controls, there was the appearance of more macrophages with large vacuoles at the periphery of the nerve (Fig 5A and 5B).

Two weeks after optic nerve injury and CNTF treatment, large numbers of cells were still present within the optic nerve, both peripherally (Fig 6A–6C) and centrally (Fig 6D–6F). Some were very large (Fig 6D) and probably were indeed macrophages, while others were smaller in size (Fig 6E) and may represent microglia. Compared to PBS controls at this stage, the more numerous cells in CNTF-treated nerves still showed signs of ongoing phagocytosis, containing vacuoles with axonal debris and multilamellar myelin/membrane remnants, as well as the numerous lipid inclusions seen at 2 w in PBS controls. Some of these cells also contained small dark membrane-bound structures that resemble secretory granules (Fig 6A and 6D).

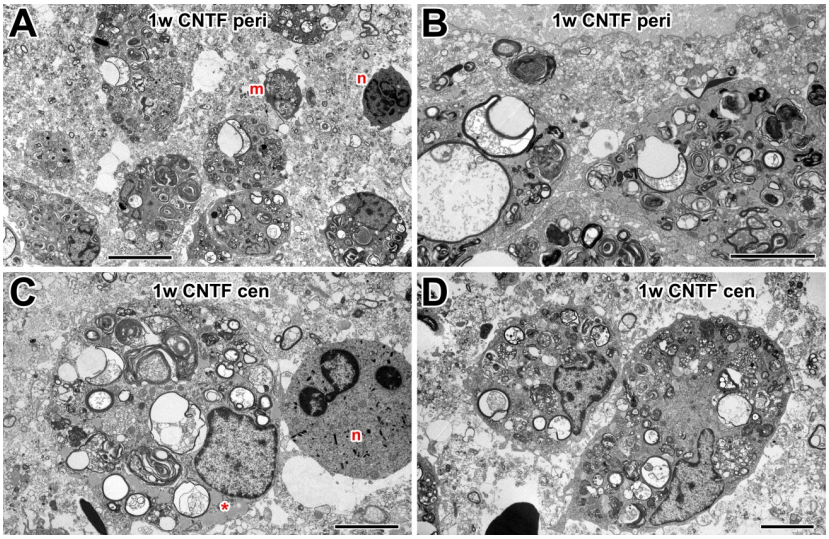

Fig 5. Electron microscopy of macrophages in 1 w CNTF-treated nerve. (A) Low power electron micrograph of the optic nerve periphery, showing numerous macrophages containing large debris-filled vacuoles. Also present are smaller microglia (m) and neurotrophil-like cells (n). (B) Active macrophages, with many large vacuoles, at nerve periphery. (C) Central macrophage with multiple phagocytic vacuoles, multilamellar bodies and also lipid inclusions (asterisk). Next to it is a neutrophil-like cell (n). (D) Centrally located macrophages with numerous multilamellar and multivesicular bodies. Scale bar: 10 μm in A; 5 μm in B, C, D.

https://doi.org/10.1371/journal.pone.0209733.g005

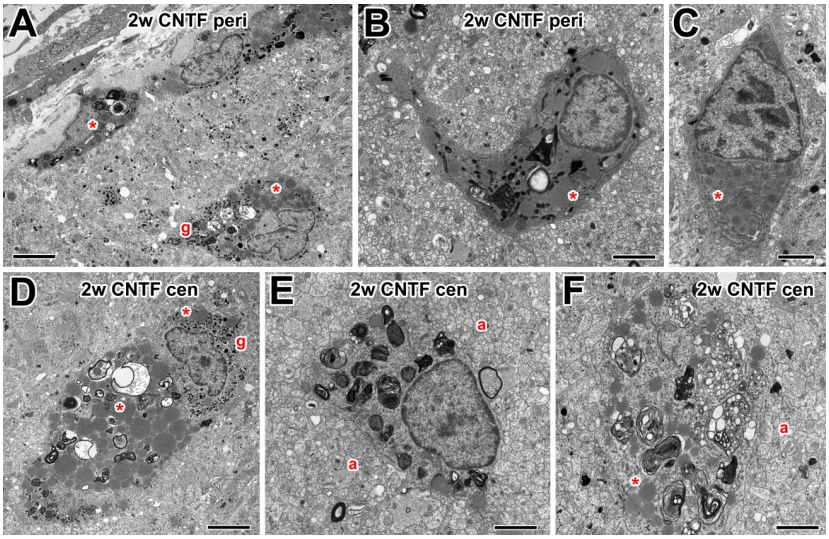

Fig 6. Electron microscopy of macrophages in 2 w CNTF-treated nerve. (A) Low power electron micrograph of the optic nerve periphery, showing macrophages containing some multilamellar bodies, also lipid inclusions (asterisks) and small dark granules (g). (B) Peripheral microglia-like cell containing multilamellar bodies and lipid inclusions (asterisk). (C) Peripheral unknown cell type containing rough endoplasmic reticulum and lipid inclusions (asterisk). (D) Large, centrally located macrophage with multilamellar bodies, vacuoles containing axonal debris, and lipid inclusions (asterisks). Around its nucleus are numerous dark granules (g). (E) Central macrophage/microglia with multilamellar bodies, in close proximity to many small axons (a). (F) Macrophage with multilamellar bodies and lipid inclusions, in proximity to axons (a). Scale bar: 5 μm in A, D; 2 μm in B, C, E, F.

https://doi.org/10.1371/journal.pone.0209733.g006

Effects of FGF-2 treatment on macrophage ultrastructure

One week after optic nerve injury and treatment with FGF-2, as with CNTF, large numbers of active macrophages were observed in the optic nerve (Fig 7A and 7B). These contained vacuoles with axonal debris and multivesicular/multilamellar bodies. Other types of blood cells, such as eosinophils, were occasionally found (Fig 7A). At two weeks after FGF-2 treatment, fewer macrophages were present in the optic nerve, similar to controls. Those that were found were large, contained numerous lipid inclusions (see above) (Fig 7C–7E), and some had multilamellar bodies and dark (possibly secretory) granules (Fig 7D).

Quantitative analysis of phagocytic organelle distributions

In order to confirm the preceding qualitative impressions of the amount of phagocytic activity, we carried out a quantitative analysis of the relative areas occupied by phagocytic vacuoles, multilamellar/multivesicular bodies and lipid inclusions, in 230 cells from 3 experimental animals per group. The total area of each type of organelle per cell was expressed as a percentage of the total area of all the organelles, thus standardizing for variations caused by different cell profile sizes, oblique sections, and partial image cropping. Rather than carry out a multivariate analysis, the phagocytic vacuoles and multilamellar bodies were initially grouped together as "phagocytic organelles", so as to compare them with the distribution of lipid inclusions (Fig 8A).

This analysis showed that at 1 week after axotomy, in all three conditions, the great majority of macrophage-like cells contain predominantly "phagocytic organelles" rather than lipid inclusions. At two weeks, on the other hand, PBS controls showed a mixture of cell types, with a large population containing few "phagocytic organelles" and predominantly lipid inclusions,

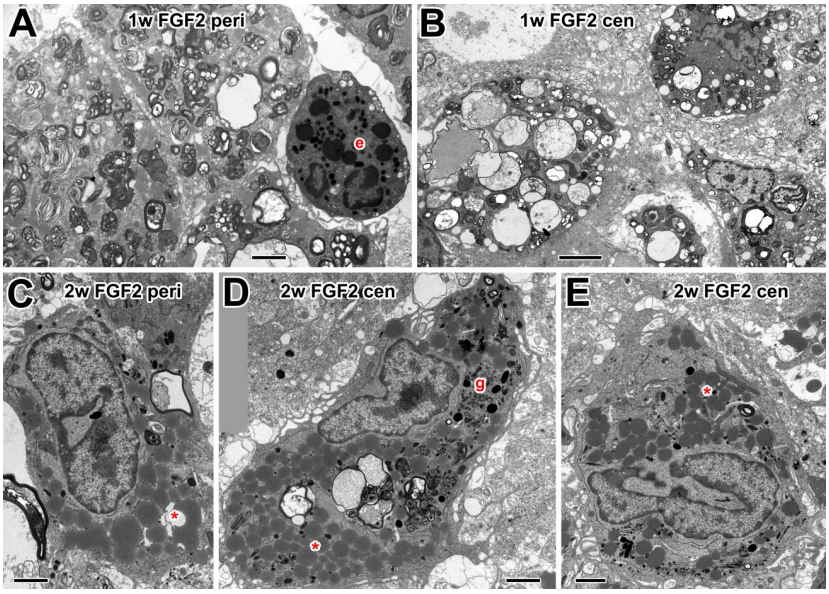

Fig 7. Electron microscopy of macrophages in FGF-2-treated nerve. (A) Peripheral macrophages at 1w, containing multilamellar bodies. Also present is a possible granulocyte, with a bilobed nucleus and dark granules (e). (B) Macrophages in the central optic nerve at 1w, containing vacuoles with axonal debris. (C) Peripheral nerve at two weeks showing macrophage with lipid inclusions (asterisk). (D) Large, centrally located macrophage at 2 w with multilamellar bodies, axonal debris and lipid inclusions (asterisks). Around its nucleus are numerous dark granules (g). (E) A similar large central macrophage with a highly indented nucleus and lipid inclusions (asterisk). Scale bar: 2 μm.

https://doi.org/10.1371/journal.pone.0209733.g007

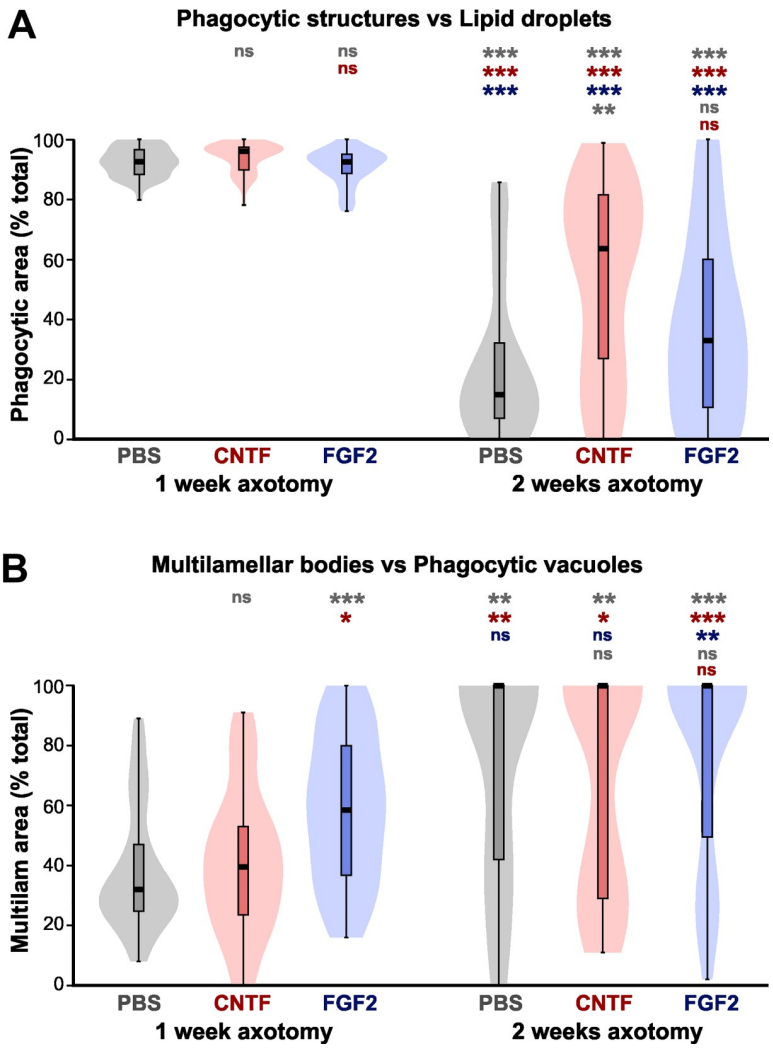

Fig 8. CNTF treatment prolongs phagocytic activity. Kernel density ("violin") plots with superimposed box-whisker plots of organelle areas, expressed as a percentage of the total organelle area. Asterisks or "ns" above each column indicate the significance when compared to PBS (rows 1 and 4, gray), CNTF (rows 2 and 5, red), or FGF2 (row 3, blue) with ANOVA and *post-hoc* Mann-Whitney comparisons using Bonferroni p-correction ($^{*}P < 0.05$, $^{**}P < 0.01$, $^{***}P < 0.001$). (A) Comparison of relative areas occupied by "phagocytic organelles" (vacuoles + multilamellar bodies) versus lipid inclusions. At one week, the majority of cells are predominantly occupied by "phagocytic organelles" as opposed to lipid inclusions. At two weeks most cells are occupied predominantly by lipid inclusions in PBS controls, but there is a significant increase in phagocytic cells with CNTF treatment. N (cells) = 42, 42, 36, 24, 41, 43. (B) Comparison of relative areas occupied by multilamellar bodies versus phagocytic vacuoles (combined as "phagocytic organelles" in Fig 8A). At one week after FGF2 treatment, there is a significant increase in the median area occupied by multilamellar bodies. At two weeks most cells are occupied by multilamellar bodies, although smaller populations remain with phagocytic vacuoles. N (cells) = 42, 42, 36, 19, 39, 34.

https://doi.org/10.1371/journal.pone.0209733.g008

and a smaller population containing more evidence of ongoing phagocytosis. The kernel density ("violin") plots indicate the presence of two cell populations with a division at about 50% phagocytic:50% lipid area. Applying this cutoff, 79% of the cells analyzed contained predominantly lipid inclusions, versus 21% with phagocytic organelles. FGF2-treated animals at 2 weeks showed no significant difference in the median phagocytic area although the population spread appeared wider (Fig 8A). CNTF treatment, however, showed a significant increase in the population of cells that had more area occupied by phagocytic organelles than lipid

inclusions. Applying the 50:50 cutoff between populations indicated that 61% of cells fall in this category (Fig 8A). This result supports our qualitative observations (see above) that there is more evidence of ongoing phagocytosis persisting at two weeks in CNTF-treated animals.

We then analyzed the relative distribution of the two "phagocytic organelle" types that were previously grouped together; namely, the large debris-containing vacuoles, which presumably indicate the relatively recent occurrence of phagocytosis, and the multilamellar or multivesicular bodies, which probably represent a later stage of debris processing (Fig 8B). At one week after axotomy, CNTF treatment showed no significant difference from PBS controls, with most cells having a larger area occupied by phagocytic vacuoles than by multilamellar bodies. Again applying the somewhat arbitrary 50:50 cutoff between the populations gave 80% of cells that are predominantly vacuolar in PBS animals, and 67% in CNTF animals. However, FGF-2 treatment significantly increases the proportion of cells that have more multilamellar bodies (Fig 8B), thus only 24% have more than 50% phagocytic vacuoles. If multilamellar bodies represent a more advanced stage of phagocytotic processing, this result implies that FGF2 treatment may accelerate this process.

By two weeks, the great majority of cells exhibited a preponderance of multilamellar bodies over phagocytic vacuoles, although there persisted a smaller cell population that had more of the latter (Fig 8B). The respective >50% vacuolar cell counts were: PBS 32%, CNTF 44%, and FGF2 24%. There were however no significant differences between the medians of the organelle distributions between PBS, CNTF or FGF2 treatments.

Discussion

Early work from this laboratory and others noted the appearance of macrophages in the axotomized optic nerve of the frog *Rana pipiens* [44,49]. However, this present study is the first detailed characterization of those macrophages, investigating the timing of their appearance after axotomy and their heterogeneity of their subpopulations. In addition, here we also investigate how the growth factors CNTF and FGF-2, which we have shown to affect the speed and the number of regenerating axons [43], also affect the macrophage populations during optic nerve regeneration.

Light microscope counts of macrophage-like cell profiles showed the appearance of many cells in the regenerating region by 1 week after injury, the numbers of which subsequently declined by half at 2 weeks. This result is consistent with our earlier qualitative report [44], in which the nerve was cut and the stumps separated. Macrophages in other animals show similar large yet transient influxes after nerve injury, for example rat sciatic nerve [50], axolotl spinal cord and peripheral axons [51], and the optic nerves of rat, goldfish and *Xenopus* tadpoles [52–54].

In the absence of specific microglial markers we cannot be absolutely sure that the smallest cell profiles identified in the light microscope are not intrinsic microglia rather than peripherally-derived macrophages. However, mammalian microglia have a maximal soma diameter of about 16 μm, with most being about 8 μm [55]. In our electron microscope images we can occasionally tentatively identify microglia from their smaller (<10 μm) size (eg. Figs 4E and 5A). However, our light microscope counts did not include cells with a Feret diameter of less than 10 μm, and the 10–20 μm category makes up only a small number of the total population (Fig 2). We are therefore confident that the majority of cells in our analysis represent macrophages.

We found that application of CNTF to the lesion doubled the number of macrophages in the nerve without affecting their size distribution, and that this effect persisted for 2 weeks after injury, long after the CNTF itself would had disappeared. There are few studies which

have investigated the possibility of such a chemoattractive effect *in vivo*, although it has been shown that the survival- and regeneration-enhancing effects of CNTF on rat RGCs depend upon the recruitment of blood-derived macrophages, and that the factor indeed has a chemotactic effect on them *in vitro* [33,56]. We also found that FGF-2 application increased the number of macrophages in the nerve, but the effect was temporary, and had disappeared by 2 weeks after injury. There are no comparable studies of FGF-2 on macrophages in other systems, however it has been shown that it increases the migration and survival of tumor-associated macrophages [57]. On the contrary, however, there appears to be increased macrophage activity after sciatic nerve injury in FGF-2-knockout mice [58].

In our previous study we investigated the effect of a single application of growth factor to the injury site on regenerating axons at 2 weeks after injury [43]. We showed that axon speed was increased 138% by CNTF and 63% by FGF-2, while axon numbers were increased 72% by FGF-2 and 52% by CNTF [43]. These prolonged effects must have far outlasted the immediate actions of the factors themselves and presumably resulted from longer-term changes in the axonal microenvironment. In the present study we investigate one such change, i.e. the increase in macrophages, and show that both CNTF and FGF-2 greatly increase the numbers of these cells, but only at 1 week after injury. The timing of these events suggests a causative effect—increased numbers of macrophages results in an enhancement of axonal growth. However, we need to test this hypothesis by inhibition of macrophages, and this will be the focus of a future study.

By what means do the macrophages enhance axonal regrowth? One obvious answer from our electron microscope observations is that they phagocytose the distal stumps of severed axons, thus removing a physical impediment to axonal elongation, which otherwise could remain in place for up to 3 months after axotomy [59]. Another possibility is that phagocytosis removes an inhibitory chemical barrier in the myelin, as in the mammalian CNS [60]. However, *Xenopus* optic tract myelin is not inhibitory to axonal extension (unlike that from the spinal cord)[61], despite both expressing an ortholog of Nogo [62]. It is more likely that, as in fish [5,63,64], the relatively few frog oligodendrocytes and their myelin are not inhibitory.

At 1 week after injury, irrespective of growth factor treatment, most macrophages were observed to have large vacuoles containing what appeared to be axon fragments, and multilamellar bodies that may represent myelin debris. By 2 weeks, in PBS- and FGF-2-treated preparations the remaining macrophages tended to contain what appeared to be lipid inclusions (not bounded by a membrane). Similar lipid inclusions, which probably represent the end points of myelin and membrane destruction, are seen in *Xenopus* astrocytes during the extensive myelin remodeling that takes place during metamorphosis [65]. More significantly, they are also the hallmark of the so-called "foamy" macrophages seen in the injured mouse spinal cord after the accumulation of excessive myelin debris [66]. These PBS- and FGF-2-treated macrophages may therefore be in the final stages of phagocytosis, while in CNTF-treated nerves the more numerous macrophages still showed signs of ongoing phagocytosis, in addition to the lipid inclusions. This apparent extension of the active phagocytic period, along with the overall higher numbers of macrophages, appears to be beneficial to axonal extension. Another possibility is that the cells themselves secrete growth-promoting substances, as is the case with mouse M2 macrophages [28], which have increased expression of, for example, insulin-like growth factor 1 and 2 and hepatocyte growth factor [67].

Early studies gave rise to ambiguous conclusions regarding the beneficial or harmful effects of macrophages on CNS repair after injury. However, in 2009 it was demonstrated that the entry of different macrophage subsets into the injured rat spinal cord, either "classically activated" proinflammatory (M1) or "alternatively activated" anti-inflammatory (M2) [68], had different effects, the former being neurotoxic while the latter promoted regeneration [28]. The

predominance of the M1 type over the M2 was postulated to be one of the factors responsible for poor CNS regenerative capabilities [22,28]. Macrophage polarization into M1/M2-like phenotypes, although undoubtedly a somewhat oversimplified classification [69], appears to be conserved throughout the vertebrates [70]. One of the distinguishing traits of the M2-like phenotype is the expression of arginase, which is purported to have healing functions [71]. Using double immunostaining of a putative pan-macrophage marker (ED1) along with an antibody against arginase (Arg1), we found that the majority (80%) of macrophages that entered the crushed frog optic nerve were Arg1+, and therefore presumably of the M2 phenotype.

Application of CNTF or FGF-2 greatly increased the overall macrophage numbers without altering the proportion of M2-like cells. Since we have shown previously that both CNTF and FGF-2 increase the numbers and speed of axons that are regenerating through the frog nerve [43] it is clear that the increased presence of M2-type macrophages is entirely consistent with them having a beneficial effect on axonal regrowth, similar to that proposed in rat [28].

Phagocytosis is, by definition, the morphological hallmark of the macrophage; however, it is not clear from the literature whether macrophage polarization is related to phagocytic activity. M1 macrophages in wounds have been described as highly phagocytic, in contrast to the M2 phenotype which accelerate wound closure [72]. On the other hand, in recent *in vitro* assays, it was shown that macrophages activated by IL-4 or IL-10 (equivalent to M2) showed higher levels of phagocytic activity compared to those activated by IFN- ((equivalent to M1) [73,74]. Our electron microscope results clearly show intense phagocytic activity in all of the macrophages that we examined, particularly at 1 week after axotomy, with or without growth factor treatment. Since we estimate that 80% of frog macrophages are Arg1-positive, and thus correspond to the M2 subtype, our results support the idea that M2 macrophages *in vivo* are phagocytically active, and that this activity is beneficial for axonal regrowth.

Our current work shows that the macrophage population in the frog optic nerve is more diverse than previously thought. This system, in which the optic nerve can regenerate, provides a good model to further study the roles of these populations in modulating axonal regeneration and ganglion cell survival.

Supporting information

S1 Table. Preliminary cell counts along nerve.
(XLSX)

S2 Table. Light microscope cell analysis data.
(XLSX)

S3 Table. Immunostaining analysis data.
(XLSX)

S4 Table. Phagocytic organelle area analysis.
(XLSX)

Author Contributions

Conceptualization: Rosa E. Blanco.

Formal analysis: Jonathan M. Blagburn.

Funding acquisition: Rosa E. Blanco.

Investigation: Giam S. Vega-Meléndez, Valeria De La Rosa-Reyes, Clarissa del Cueto.

Methodology: Rosa E. Blanco, Giam S. Vega-Meléndez.

Project administration: Rosa E. Blanco.

Supervision: Rosa E. Blanco.

Visualization: Jonathan M. Blagburn.

Writing – original draft: Rosa E. Blanco, Giam S. Vega-Meléndez, Jonathan M. Blagburn.

Writing – review & editing: Rosa E. Blanco, Jonathan M. Blagburn.

References

1. Lewin GR, Barde YA. Physiology of the neurotrophins. Annu Rev Neurosci. 1996; 19: 289–317. Available: http://www.ncbi.nlm.nih.gov/entrez/query.fcgi?cmd=Retrieve&db=PubMed&dopt=Citation&list_uids=8833445 https://doi.org/10.1146/annurev.ne.19.030196.001445 PMID: 8833445
2. Villegas-Perez MP, Vidal-Sanz M, Rasminsky M, Bray GM, Aguayo AJ. Rapid and protracted phases of retinal ganglion cell loss follow axotomy in the optic nerve of adult rats. J Neurobiol. 1993; 24: 23–36. Available: http://www.ncbi.nlm.nih.gov/entrez/query.fcgi?cmd=Retrieve&db=PubMed&dopt=Citation&list_uids=8419522 https://doi.org/10.1002/neu.480240103 PMID: 8419522
3. David S, Aguayo AJ. Axonal elongation into peripheral nervous system "bridges" after central nervous system injury in adult rats. Science (80-). 1981; 214: 931–933. Available: http://www.ncbi.nlm.nih.gov/entrez/query.fcgi?cmd=Retrieve&db=PubMed&dopt=Citation&list_uids=6171034 PMID: 6171034
4. Schwab ME. Increasing plasticity and functional recovery of the lesioned spinal cord. Prog Brain Res. 2002; 137: 351–359. Available: http://www.ncbi.nlm.nih.gov/entrez/query.fcgi?cmd=Retrieve&db=PubMed&dopt=Citation&list_uids=12440377 PMID: 12440377
5. Wanner M, Lang DM, Bandtlow CE, Schwab ME, Bastmeyer M, Stuermer CA. Reevaluation of the growth-permissive substrate properties of goldfish optic nerve myelin and myelin proteins. J Neurosci. 1995; 15: 7500–7508. Available: http://www.ncbi.nlm.nih.gov/entrez/query.fcgi?cmd=Retrieve&db=PubMed&dopt=Citation&list_uids=7472501 PMID: 7472501
6. Ghosh S, Hui SP. Axonal regeneration in zebrafish spinal cord. Regeneration. 2018; 5: 43–60. https://doi.org/10.1002/reg2.99 PMID: 29721326
7. Scalia F, Arango V, Singman EL. Loss and displacement of ganglion cells after optic nerve regeneration in adult Rana pipiens. Brain Res. 1985; 344: 267–280. Available: http://www.ncbi.nlm.nih.gov/entrez/query.fcgi?cmd=Retrieve&db=PubMed&dopt=Citation&list_uids=3876140 PMID: 3876140
8. Snider WD. Functions of the neurotrophins during nervous system development: what the knockouts are teaching us. Cell. 1994; 77: 627–638. Available: http://www.ncbi.nlm.nih.gov/entrez/query.fcgi?cmd=Retrieve&db=PubMed&dopt=Citation&list_uids=8205613 PMID: 8205613
9. Thoenen H. Neurotrophins and neuronal plasticity. Science (80-). 1995; 270: 593–598. Available: http://www.ncbi.nlm.nih.gov/entrez/query.fcgi?cmd=Retrieve&db=PubMed&dopt=Citation&list_uids=7570017 PMID: 7570017
10. von Bartheld CS. Neurotrophins in the developing and regenerating visual system. Histol Histopathol. 1998; 13: 437–459. Available: http://www.ncbi.nlm.nih.gov/entrez/query.fcgi?cmd=Retrieve&db=PubMed&dopt=Citation&list_uids=9589902 https://doi.org/10.14670/HH-13.437 PMID: 9589902
11. Di Polo A, Aigner LJ, Dunn RJ, Bray GM, Aguayo AJ. Prolonged delivery of brain-derived neurotrophic factor by adenovirus-infected Muller cells temporarily rescues injured retinal ganglion cells. Proc Natl Acad Sci U S A. 1998; 95: 3978–3983. Available: http://www.ncbi.nlm.nih.gov/entrez/query.fcgi?cmd=Retrieve&db=PubMed&dopt=Citation&list_uids=9520478 PMID: 9520478
12. Pease ME, Zack DJ, Berlinicke C, Bloom K, Cone F, Wang Y, et al. Effect of CNTF on retinal ganglion cell survival in experimental glaucoma. Invest Ophthalmol Vis Sci. NIH Public Access; 2009; 50: 2194–200. https://doi.org/10.1167/iovs.08-3013 PMID: 19060281
13. Blanco RE, Lopez-Roca A, Soto J, Blagburn JM. Basic fibroblast growth factor applied to the optic nerve after injury increases long-term cell survival in the frog retina. J Comp Neurol. 2000; 423: 646–658. Available: http://www.ncbi.nlm.nih.gov/entrez/query.fcgi?cmd=Retrieve&db=PubMed&dopt=Citation&list_uids=10880994 PMID: 10880994
14. Welsbie DS, Mitchell KL, Jaskula-Ranga V, Sluch VM, Yang Z, Kim J, et al. Enhanced Functional Genomic Screening Identifies Novel Mediators of Dual Leucine Zipper Kinase-Dependent Injury Signaling in Neurons. Neuron. 2017; 94: 1142–1154.e6. https://doi.org/10.1016/j.neuron.2017.06.008 PMID: 28641113

15. Liddelow SA, Guttenplan KA, Clarke LE, Bennett FC, Bohlen CJ, Schirmer L, et al. Neurotoxic reactive astrocytes are induced by activated microglia. Nature. 2017; 541: 481–487. https://doi.org/10.1038/nature21029 PMID: 28099414

16. Li Y, Andereggen L, Yuki K, Omura K, Yin Y, Gilbert H-Y, et al. Mobile zinc increases rapidly in the retina after optic nerve injury and regulates ganglion cell survival and optic nerve regeneration. Proc Natl Acad Sci. 2017; 114: E209–E218. https://doi.org/10.1073/pnas.1616811114 PMID: 28049831

17. Bogie JFJ, Stinissen P, Hendriks JJA. Macrophage subsets and microglia in multiple sclerosis. Acta Neuropathol. 2014; 128: 191–213. https://doi.org/10.1007/s00401-014-1310-2 PMID: 24952885

18. Ulland TK, Song WM, Huang SC-C, Ulrich JD, Sergushichev A, Beatty WL, et al. TREM2 Maintains Microglial Metabolic Fitness in Alzheimer's Disease. Cell. 2017; 170: 649–663.e13. https://doi.org/10.1016/j.cell.2017.07.023 PMID: 28802038

19. Lecours C, Bordeleau M, Cantin L, Parent M, Paolo T Di, Tremblay M-È. Microglial Implication in Parkinson's Disease: Loss of Beneficial Physiological Roles or Gain of Inflammatory Functions? Front Cell Neurosci. 2018; 12: 282. https://doi.org/10.3389/fncel.2018.00282 PMID: 30214398

20. Minagar A, Shapshak P, Fujimura R, Ownby R, Heyes M, Eisdorfer C. The role of macrophage/microglia and astrocytes in the pathogenesis of three neurologic disorders: HIV-associated dementia, Alzheimer disease, and multiple sclerosis. J Neurol Sci. 2002; 202: 13–23. Available: http://www.ncbi.nlm.nih.gov/pubmed/12220687 PMID: 12220687

21. Kong X, Gao J. Macrophage polarization: a key event in the secondary phase of acute spinal cord injury. J Cell Mol Med. 2017; 21: 941–954. https://doi.org/10.1111/jcmm.13034 PMID: 27957787

22. Gensel JC, Zhang B. Macrophage activation and its role in repair and pathology after spinal cord injury. Brain Res. 2015; 1619: 1–11. https://doi.org/10.1016/j.brainres.2014.12.045 PMID: 25578260

23. Greenhalgh AD, Zarruk JG, Healy LM, Baskar Jesudasan SJ, Jhelum P, Salmon CK, et al. Peripherally derived macrophages modulate microglial function to reduce inflammation after CNS injury. Daneman R, editor. PLOS Biol. 2018; 16: e2005264. https://doi.org/10.1371/journal.pbio.2005264 PMID: 30332405

24. van Furth R, Cohn ZA. The origin and kinetics of mononuclear phagocytes. J Exp Med. 1968; 128: 415–35. Available: http://www.ncbi.nlm.nih.gov/pubmed/5666958 PMID: 5666958

25. Gordon S, Taylor PR. Monocyte and macrophage heterogeneity. Nat Rev Immunol. 2005; 5: 953–964. https://doi.org/10.1038/nri1733 PMID: 16322748

26. Lindborg JA, Mack M, Zigmond RE. Neutrophils Are Critical for Myelin Removal in a Peripheral Nerve Injury Model of Wallerian Degeneration. J Neurosci. 2017; 37: 10258–10277. https://doi.org/10.1523/JNEUROSCI.2085-17.2017 PMID: 28912156

27. Barrette B, Hebert M-A, Filali M, Lafortune K, Vallieres N, Gowing G, et al. Requirement of Myeloid Cells for Axon Regeneration. J Neurosci. 2008; 28: 9363–9376. https://doi.org/10.1523/JNEUROSCI.1447-08.2008 PMID: 18799670

28. Kigerl KA, Gensel JC, Ankeny DP, Alexander JK, Donnelly DJ, Popovich PG. Identification of two distinct macrophage subsets with divergent effects causing either neurotoxicity or regeneration in the injured mouse spinal cord. J Neurosci. 2009; 29: 13435–13444. https://doi.org/10.1523/JNEUROSCI.3257-09.2009 PMID: 19864556

29. London A, Cohen M, Schwartz M. Microglia and monocyte-derived macrophages: functionally distinct populations that act in concert in CNS plasticity and repair. Front Cell Neurosci. 2013; 7: 34. https://doi.org/10.3389/fncel.2013.00034 PMID: 23596391

30. Leon S, Yin Y, Nguyen J, Irwin N, Benowitz LI. Lens injury stimulates axon regeneration in the mature rat optic nerve. J Neurosci. 2000; 20: 4615–26. Available: http://www.ncbi.nlm.nih.gov/pubmed/10844031 PMID: 10844031

31. Yin Y, Cui Q, Li Y, Irwin N, Fischer D, Harvey AR, et al. Macrophage-derived factors stimulate optic nerve regeneration. J Neurosci. 2003; 23: 2284–93. Available: http://www.ncbi.nlm.nih.gov/pubmed/12657687 PMID: 12657687

32. Fischer D, Heiduschka P, Thanos S. Lens-Injury-Stimulated Axonal Regeneration throughout the Optic Pathway of Adult Rats. Exp Neurol. 2001; 172: 257–272. https://doi.org/10.1006/exnr.2001.7822 PMID: 11716551

33. Cen L-P, Luo J-M, Zhang C-W, Fan Y-M, Song Y, So K-F, et al. Chemotactic effect of ciliary neurotrophic factor on macrophages in retinal ganglion cell survival and axonal regeneration. Invest Ophthalmol Vis Sci. 2007; 48: 4257–66. https://doi.org/10.1167/iovs.06-0791 PMID: 17724215

34. Zigmond RE, Echevarria FD. Macrophage biology in the peripheral nervous system after injury. Prog Neurobiol. 2019; 173: 102–121. https://doi.org/10.1016/j.pneurobio.2018.12.001 PMID: 30579784

35. Niemi JP, DeFrancesco-Lisowitz A, Cregg JM, Howarth M, Zigmond RE. Overexpression of the monocyte chemokine CCL2 in dorsal root ganglion neurons causes a conditioning-like increase in neurite

outgrowth and does so via a STAT3 dependent mechanism. Exp Neurol. 2016; 275: 25–37. https://doi.org/10.1016/j.expneurol.2015.09.018 PMID: 26431741

36. Kwon MJ, Shin HY, Cui Y, Kim H, Thi AHL, Choi JY, et al. CCL2 Mediates Neuron-Macrophage Interactions to Drive Proregenerative Macrophage Activation Following Preconditioning Injury. J Neurosci. 2015; 35: 15934–15947. https://doi.org/10.1523/JNEUROSCI.1924-15.2015 PMID: 26631474

37. Hilla AM, Diekmann H, Fischer D. Microglia Are Irrelevant for Neuronal Degeneration and Axon Regeneration after Acute Injury. J Neurosci. 2017; 37: 6113–6124. https://doi.org/10.1523/JNEUROSCI.0584-17.2017 PMID: 28539419

38. Bollaerts I, Van Houcke J, Andries L, De Groef L, Moons L. Neuroinflammation as Fuel for Axonal Regeneration in the Injured Vertebrate Central Nervous System. Mediators Inflamm. 2017; 2017: 9478542. https://doi.org/10.1155/2017/9478542 PMID: 28203046

39. Soto I, Marie B, Baro DJ, Blanco RE. FGF-2 modulates expression and distribution of GAP-43 in frog retinal ganglion cells after optic nerve injury. J Neurosci Res. 2003; 73: 507–517. Available: http://www.ncbi.nlm.nih.gov/entrez/query.fcgi?cmd=Retrieve&db=PubMed&dopt=Citation&list_uids=12898535 https://doi.org/10.1002/jnr.10673 PMID: 12898535

40. Blanco RE, Soto I, Duprey-Díaz M, Blagburn JM. Up-regulation of brain-derived neurotrophic factor by application of fibroblast growth factor-2 to the cut optic nerve is important for long-term survival of retinal ganglion cells. J Neurosci Res. 2008;86. https://doi.org/10.1002/jnr.21793 PMID: 18655198

41. Duprey-Díaz MV, Blagburn JM, Blanco RE. Changes in fibroblast growth factor-2 and FGF receptors in the frog visual system during optic nerve regeneration. J Chem Neuroanat. 2012; 46: 35–44. https://doi.org/10.1016/j.jchemneu.2012.08.003 PMID: 22940608

42. Ríos-Muñoz W, Soto I, Duprey-Díaz M V, Blagburn JM, Blanco RE. Fibroblast growth factor 2 applied to the optic nerve after axotomy increases Bcl-2 and decreases Bax in ganglion cells by activating the ERK signaling pathway. J Neurochem. Blackwell Science Ltd; 2005; 93: 1422–1433. https://doi.org/10.1111/j.1471-4159.2005.03129.x PMID: 15935058

43. Vega-Meléndez GS, Blagburn JM, Blanco RE. Ciliary neurotrophic factor and fibroblast growth factor increase the speed and number of regenerating axons after optic nerve injury in adult Rana pipiens. J Neurosci Res. 2014;92. https://doi.org/10.1002/jnr.23303 PMID: 24166589

44. Blanco RE, Orkand PM. Astrocytes and regenerating axons at the proximal stump of the severed frog optic nerve. Cell Tissue Res. 1996; 286: 337–345. Available: http://www.ncbi.nlm.nih.gov/entrez/query.fcgi?cmd=Retrieve&db=PubMed&dopt=Citation&list_uids=8929336 PMID: 8929336

45. Micklem K, Rigney E, Cordell J, Simmons D, Stross P, Turley H, et al. A human macrophage-associated antigen (CD68) detected by six different monoclonal antibodies. Br J Haematol. 1989; 73: 6–11. Available: http://www.ncbi.nlm.nih.gov/pubmed/2803980 PMID: 2803980

46. Chistiakov DA, Killingsworth MC, Myasoedova VA, Orekhov AN, Bobryshev Y V. CD68/macrosialin: not just a histochemical marker. Lab Investig. 2017; 97: 4–13. https://doi.org/10.1038/labinvest.2016.116 PMID: 27869795

47. Riew T-R, Kim HL, Choi J-H, Jin X, Shin Y-J, Lee M-Y. Progressive accumulation of autofluorescent granules in macrophages in rat striatum after systemic 3-nitropropionic acid: a correlative light- and electron-microscopic study. Histochem Cell Biol. 2017; 148: 517–528. https://doi.org/10.1007/s00418-017-1589-x PMID: 28597061

48. Rauh MJ, Kalesnikoff J, Hughes M, Sly L, Lam V, Krystal G. Role of Src homology 2-containing-inositol 5'-phosphatase (SHIP) in mast cells and macrophages. Biochem Soc Trans. 2003; 31: 286–91. https://doi.org/10.1042/ PMID: 12546703

49. Liuzzi FJ, Miller RH. Neovascularization occurs in response to crush lesions of adult frog optic nerves. J Neurocytol. 1990; 19: 224–34. Available: http://www.ncbi.nlm.nih.gov/pubmed/1694231 PMID: 1694231

50. Taskinen HS, Röyttä M. The dynamics of macrophage recruitment after nerve transection. Acta Neuropathol. 1997; 93: 252–9. Available: http://www.ncbi.nlm.nih.gov/pubmed/9083556 PMID: 9083556

51. Zammit PS, Clarke JD, Golding JP, Goodbrand IA, Tonge DA. Macrophage response during axonal regeneration in the axolotl central and peripheral nervous system. Neuroscience. 1993; 54: 781–9. Available: http://www.ncbi.nlm.nih.gov/pubmed/8332261 PMID: 8332261

52. Morishita S, Oku H, Horie T, Tonari M, Kida T, Okubo A, et al. Systemic Simvastatin Rescues Retinal Ganglion Cells from Optic Nerve Injury Possibly through Suppression of Astroglial NF-κB Activation. Barnes S, editor. PLoS One. 2014; 9: e84387. https://doi.org/10.1371/journal.pone.0084387 PMID: 24392131

53. Battisti WP, Wang J, Bozek K, Murray M. Macrophages, microglia, and astrocytes are rapidly activated after crush injury of the goldfish optic nerve: A light electron microscopic analysis. J Comp Neurol. 1995; 354: 306–320. https://doi.org/10.1002/cne.903540211 PMID: 7540185

54. Wilson MA, Gaze RM, Goodbrand IA, Taylor JS. Regeneration in the Xenopus tadpole optic nerve is preceded by a massive macrophage/microglial response. Anat Embryol (Berl). 1992; 186: 75–89. Available: http://www.ncbi.nlm.nih.gov/pubmed/1514705

55. Kongsui R, Beynon SB, Johnson SJ, Walker FR. Quantitative assessment of microglial morphology and density reveals remarkable consistency in the distribution and morphology of cells within the healthy prefrontal cortex of the rat. J Neuroinflammation. 2014; 11: 182. https://doi.org/10.1186/s12974-014-0182-7 PMID: 25343964

56. Kobayashi H, Mizisin AP. CNTFR α alone or in combination with CNTF promotes macrophage chemotaxis in vitro. Neuropeptides. 2000; 34: 338–347. https://doi.org/10.1054/npep.2000.0829 PMID: 11162290

57. Takase N, Koma Y, Urakawa N, Nishio M, Arai N, Akiyama H, et al. NCAM- and FGF-2-mediated FGFR1 signaling in the tumor microenvironment of esophageal cancer regulates the survival and migration of tumor-associated macrophages and cancer cells. Cancer Lett. 2016; 380: 47–58. https://doi.org/10.1016/j.canlet.2016.06.009 PMID: 27317650

58. Jungnickel J, Claus P, Gransalke K, Timmer M, Grothe C. Targeted disruption of the FGF-2 gene affects the response to peripheral nerve injury. Mol Cell Neurosci. 2004; 25: 444–452. https://doi.org/10.1016/j.mcn.2003.11.007 PMID: 15033172

59. Blanco RE, Marrero H, Orkand PM, Orkand RK. Changes in ultrastructure and voltage-dependent currents at the glia limitans of the frog optic nerve following retinal ablation. Glia. 1993; 8: 97–105. Available: http://www.ncbi.nlm.nih.gov/entrez/query.fcgi?cmd=Retrieve&db=PubMed&dopt=Citation&list_uids=8406678 https://doi.org/10.1002/glia.440080205 PMID: 8406678

60. Caroni P, Schwab ME. Antibody against myelin-associated inhibitor of neurite growth neutralizes nonpermissive substrate properties of CNS white matter. Neuron. 1988; 1: 85–96. Available: http://www.ncbi.nlm.nih.gov/entrez/query.fcgi?cmd=Retrieve&db=PubMed&dopt=Citation&list_uids=3272156 PMID: 3272156

61. Lang DM, Rubin BP, Schwab ME, Stuermer CA. CNS myelin and oligodendrocytes of the Xenopus spinal cord—but not optic nerve—are nonpermissive for axon growth. J Neurosci. 1995; 15: 99–109. Available: http://www.ncbi.nlm.nih.gov/entrez/query.fcgi?cmd=Retrieve&db=PubMed&dopt=Citation&list_uids=7823155 PMID: 7823155

62. Klinger M, Diekmann H, Heinz D, Hirsch C, Hannbeck von Hanwehr S, Petrausch B, et al. Identification of two nogo/rtn4 genes and analysis of Nogo-A expression in Xenopus laevis. Mol Cell Neurosci. 2004; 25: 205–216. https://doi.org/10.1016/j.mcn.2003.09.021 PMID: 15019938

63. Bastmeyer M, Beckmann M, Schwab ME, Stuermer CA. Growth of regenerating goldfish axons is inhibited by rat oligodendrocytes and CNS myelin but not but not by goldfish optic nerve tract oligodendrocytelike cells and fish CNS myelin. J Neurosci. 1991; 11: 626–640. Available: http://www.ncbi.nlm.nih.gov/entrez/query.fcgi?cmd=Retrieve&db=PubMed&dopt=Citation&list_uids=2002357 PMID: 2002357

64. Bodrikov V, Welte C, Wiechers M, Weschenfelder M, Kaur G, Shypitsyna A, et al. Substrate properties of zebrafish Rtn4b/Nogo and axon regeneration in the zebrafish optic nerve. J Comp Neurol. 2017; 525: 2991–3009. https://doi.org/10.1002/cne.24253 PMID: 28560734

65. Mills EA, Davis CO, Bushong EA, Boassa D, Kim K-Y, Ellisman MH, et al. Astrocytes phagocytose focal dystrophies from shortening myelin segments in the optic nerve of Xenopus laevis at metamorphosis. Proc Natl Acad Sci U S A. National Academy of Sciences; 2015; 112: 10509–14. https://doi.org/10.1073/pnas.1506486112 PMID: 26240339

66. Wang X, Cao K, Sun X, Chen Y, Duan Z, Sun L, et al. Macrophages in spinal cord injury: phenotypic and functional change from exposure to myelin debris. Glia. NIH Public Access; 2015; 63: 635–51. https://doi.org/10.1002/glia.22774 PMID: 25452166

67. Tomlinson JE, Žygelytė E, Grenier JK, Edwards MG, Cheetham J. Temporal changes in macrophage phenotype after peripheral nerve injury. J Neuroinflammation. BioMed Central; 2018; 15: 185. https://doi.org/10.1186/s12974-018-1219-0 PMID: 29907154

68. Mills CD, Kincaid K, Alt JM, Heilman MJ, Hill AM. M-1/M-2 macrophages and the Th1/Th2 paradigm. J Immunol. 2000; 164: 6166–73. Available: http://www.ncbi.nlm.nih.gov/pubmed/10843666 PMID: 10843666

69. Martinez FO, Gordon S. The M1 and M2 paradigm of macrophage activation: time for reassessment. F1000Prime Rep. Faculty of 1000 Ltd; 2014; 6: 13. https://doi.org/10.12703/P6-13 PMID: 24669294

70. Edholm E-S, Rhoo KH, Robert J. Evolutionary Aspects of Macrophages Polarization. Results and problems in cell differentiation. 2017. pp. 3–22. https://doi.org/10.1007/978-3-319-54090-0_1

71. Dzik JM. Evolutionary Roots of Arginase Expression and Regulation. Front Immunol. 2014; 5: 544. https://doi.org/10.3389/fimmu.2014.00544 PMID: 25426114

72. Hesketh M, Sahin KB, West ZE, Murray RZ. Macrophage Phenotypes Regulate Scar Formation and Chronic Wound Healing. Int J Mol Sci. Multidisciplinary Digital Publishing Institute (MDPI); 2017;18. https://doi.org/10.3390/ijms18071545 PMID: 28714933

73. Mendoza-Coronel E, Ortega E. Macrophage Polarization Modulates FcγR- and CD13-Mediated Phagocytosis and Reactive Oxygen Species Production, Independently of Receptor Membrane Expression. Front Immunol. Frontiers Media SA; 2017; 8: 303. https://doi.org/10.3389/fimmu.2017.00303 PMID: 28396660

74. Kapellos TS, Taylor L, Lee H, Cowley SA, James WS, Iqbal AJ, et al. A novel real time imaging platform to quantify macrophage phagocytosis. Biochem Pharmacol. 2016; 116: 107–19. https://doi.org/10.1016/j.bcp.2016.07.011 PMID: 27475716